Supplementary Information (SI) for Food & Function.
This journal is © The Royal Society of Chemistry 2024

1. Supplementary picture

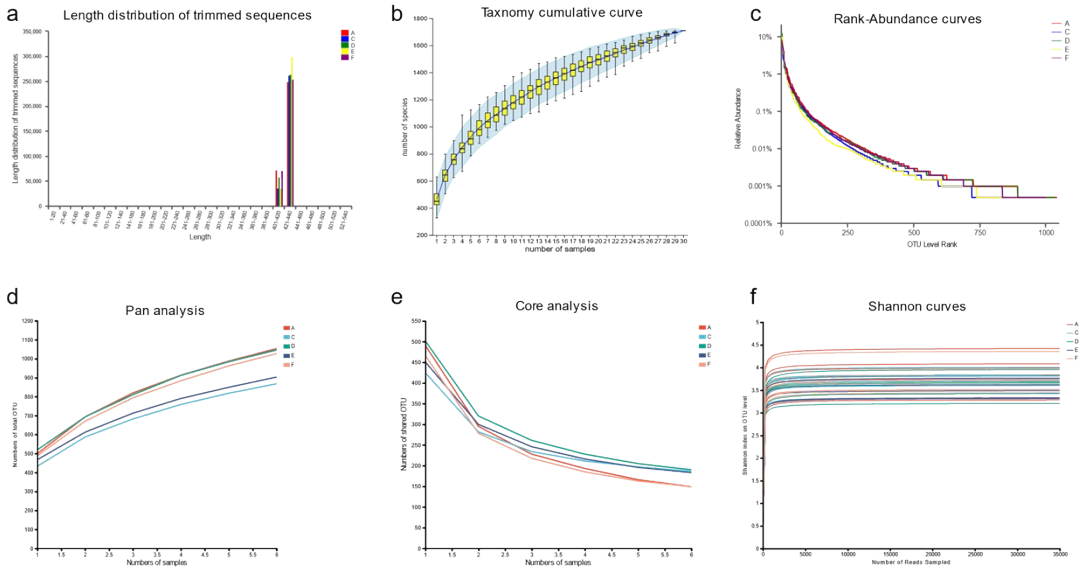

Figure 1: Sequencing information statistics and OTU species analysis. (a) Sequence length distribution graph. (b) Species accumulation curve. (c) Rank-Abundance curves. (d) Pan analysis diagram. (e) Core curve. (f) Dilution curve. A is the negative control group, C is the MPTP group, D is the ACN50+MPTP group, E is the ACN100+MPTP group, and F is the ACN200+MPTP group.

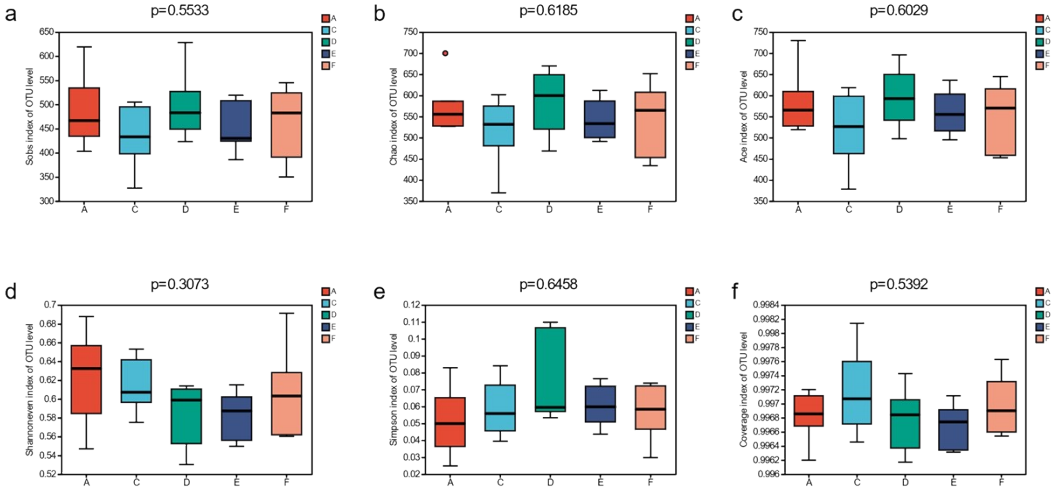

Figure 2: Alpha diversity analysis. (a) Sobs curve. (b) Chao curve. (c) Ace curve. (d) Shannoneven curve. (e) Simpson curve. (f) Coverage curve. A is the negative control group, C is the MPTP group, D is the ACN50+MPTP group, E is the ACN100+MPTP group, and F is the ACN200+MPTP group.

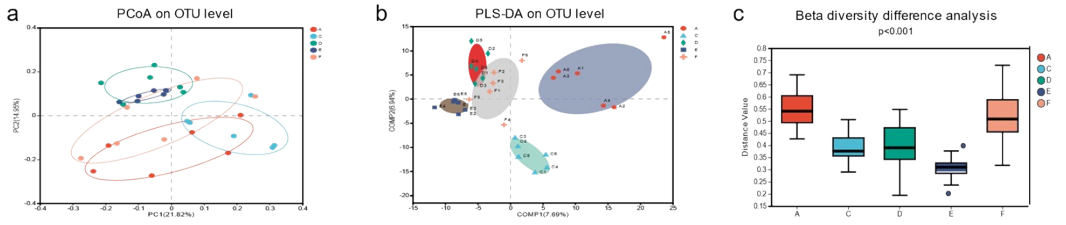

Figure 3: Beta diversity analysis. (a) PCoA plot. (b) PLS-DA plot. (c) Beta diversity intergroup difference box plot.

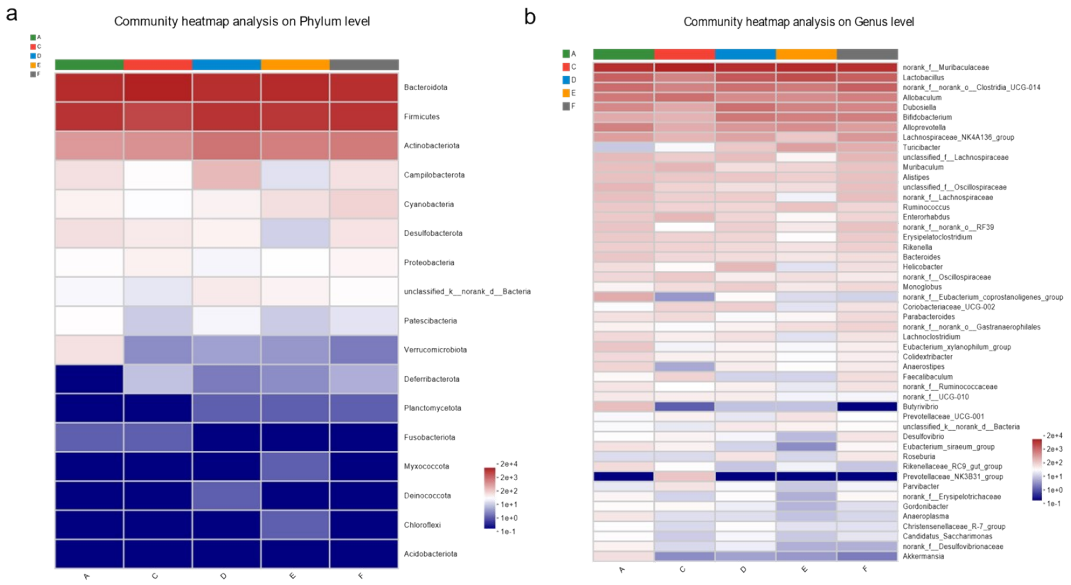

Figure 4: Heat maps of communities below the level of phylum (a) and genus (b). A is the negative control group, C is the MPTP group, D is the ACN50+MPTP group, E is the ACN100+MPTP group, and F is the ACN200+MPTP group. n=6 mice per group.

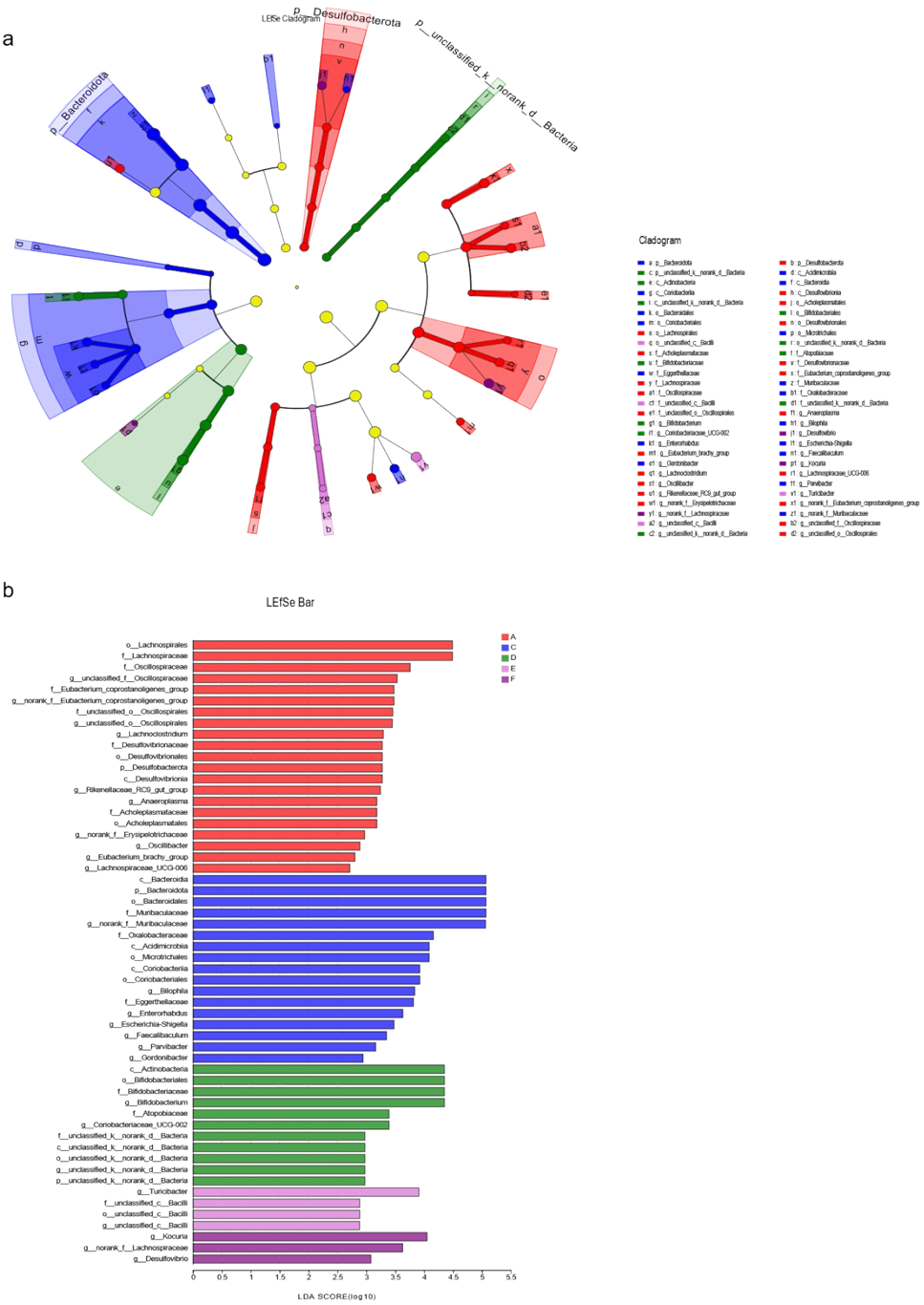

Figure 5: (a) LEfSe multi-level species hierarchy tree. (b) LDA discrimination histogram. A is the negative control group, C is the MPTP group, D is the ACN50+MPTP group, E is the ACN100+MPTP group, and F is the ACN200+MPTP group. n=6 mice per group.

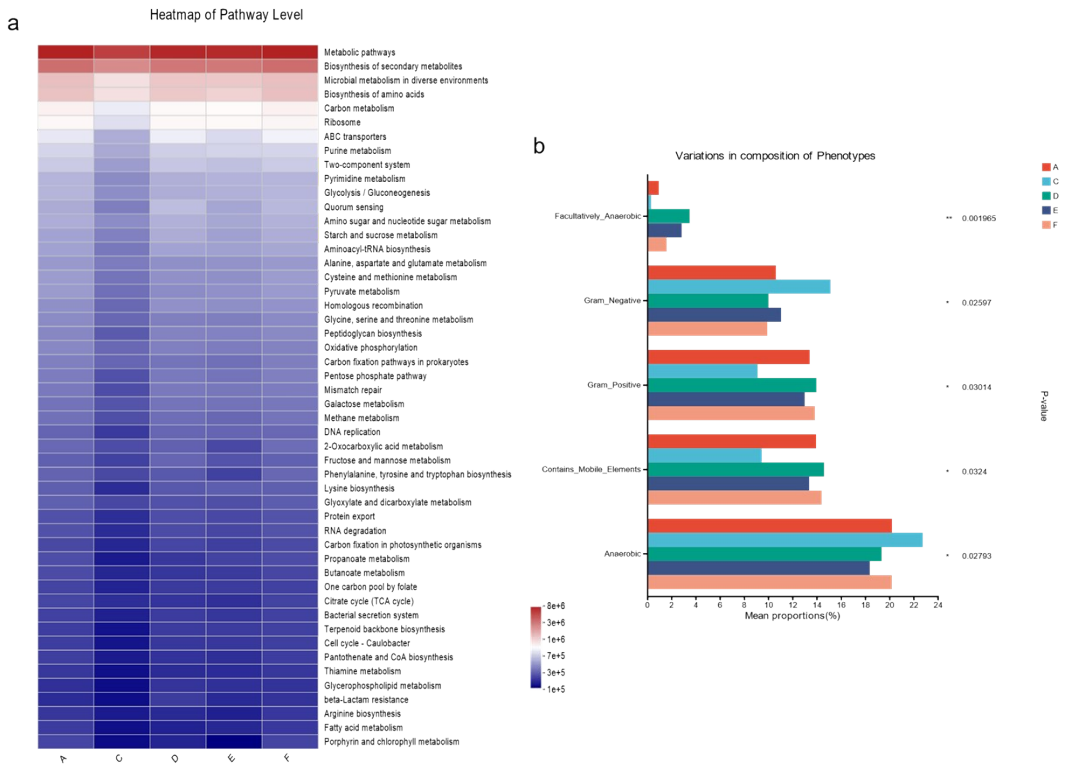

Figure 6: Effect of ACN on intestinal microbiota diversity in mice with PD-like phenotype. Relationships between samples and species at the (a) phylum and (d) genus level. Histogram of significant differences between groups at the level of (b) phylum and (e) genus. Heat maps of communities below the level of phylum (c) and genus (f). (g) LEfSe multi-level species hierarchy tree. (h) PICRUSt2 function prediction heat map. (i) Species-phenotypic contribution analysis for BugBase phenotypic prediction. A is the negative control group, C is the MPTP group, D is the ACN50+MPTP group, E is the ACN100+MPTP group, and F is the ACN200+MPTP group. n=6 mice per group.

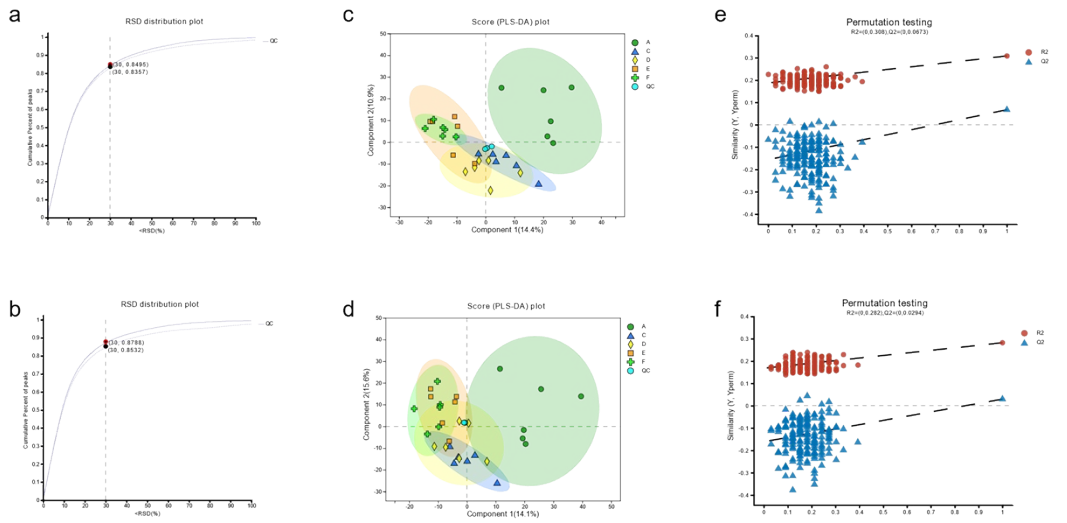

Figure 7: Analysis of urine metabolomics approach. QC sample evaluation chart under (a) pos and (b) neg, dashed line indicates before pretreatment and solid line indicates after pretreatment. (c) PLS-DA score plots of urine samples in pos and (d) neg mode. (e) PLS-DA displacement test in pos

and (f) neg mode. A is the negative control group, C is the MPTP group, D is the ACN50+MPTP group, E is the ACN100+MPTP group, and F is the ACN200+MPTP group.

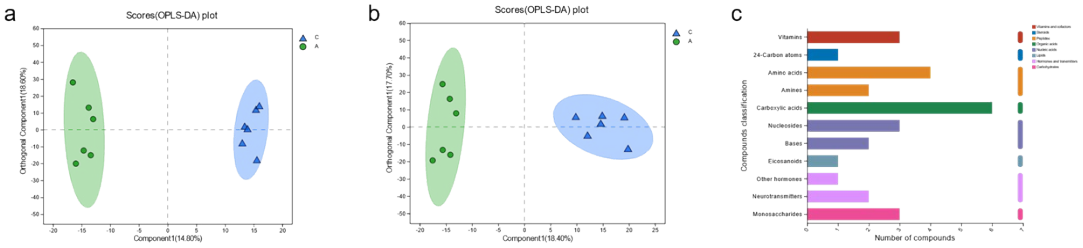

Figure 8: Urinary differential metabolite screening in mice with PD-like phenotypes. (a) Plot of OPLS-DA scores in model and control groups in pos and (b) neg mode. (c) Statistical graph of KEGG compound classification. A is the negative control group, C is the MPTP group.

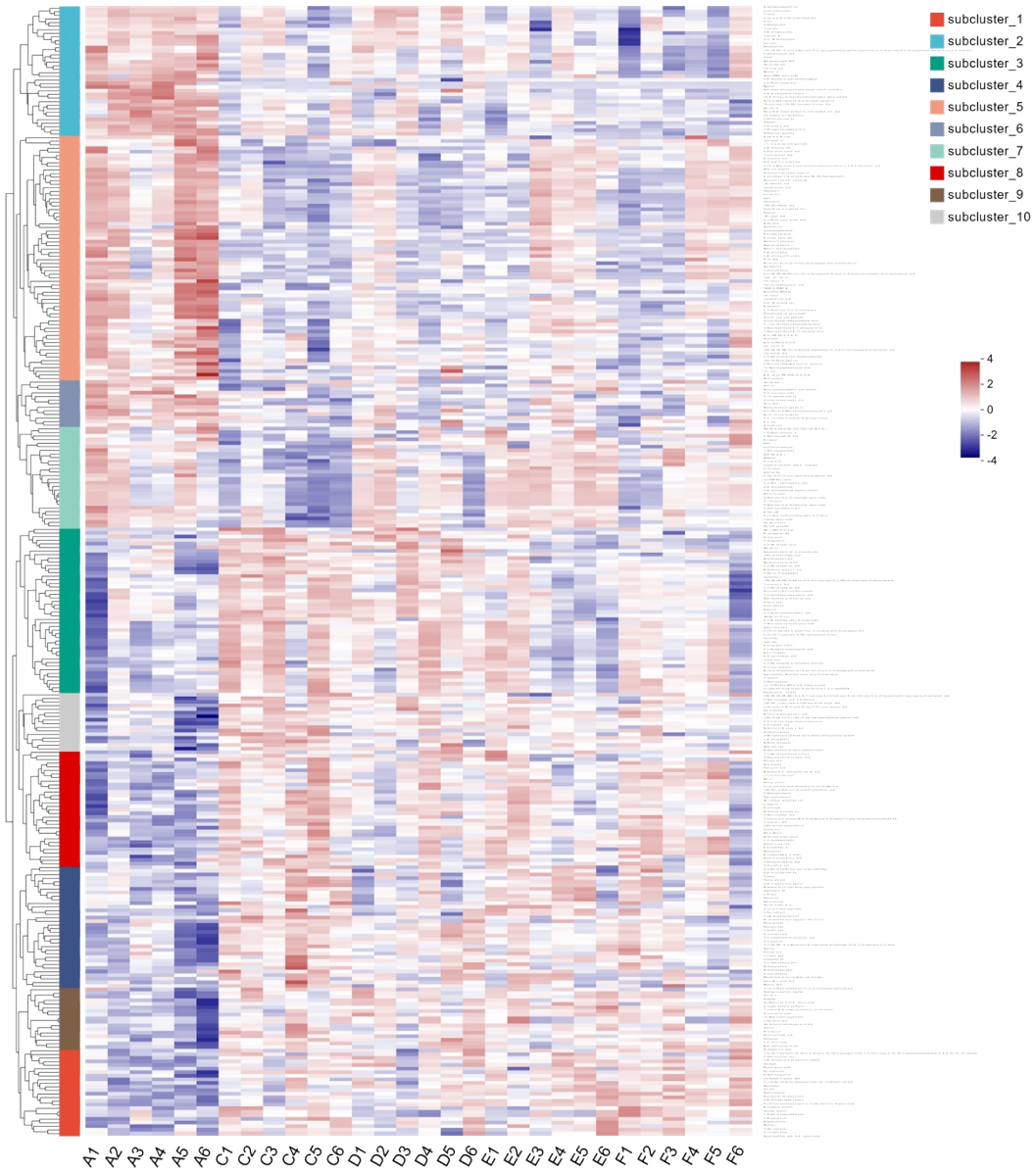

Figure 9: Clustered heatmap of PD differential urine metabolites.

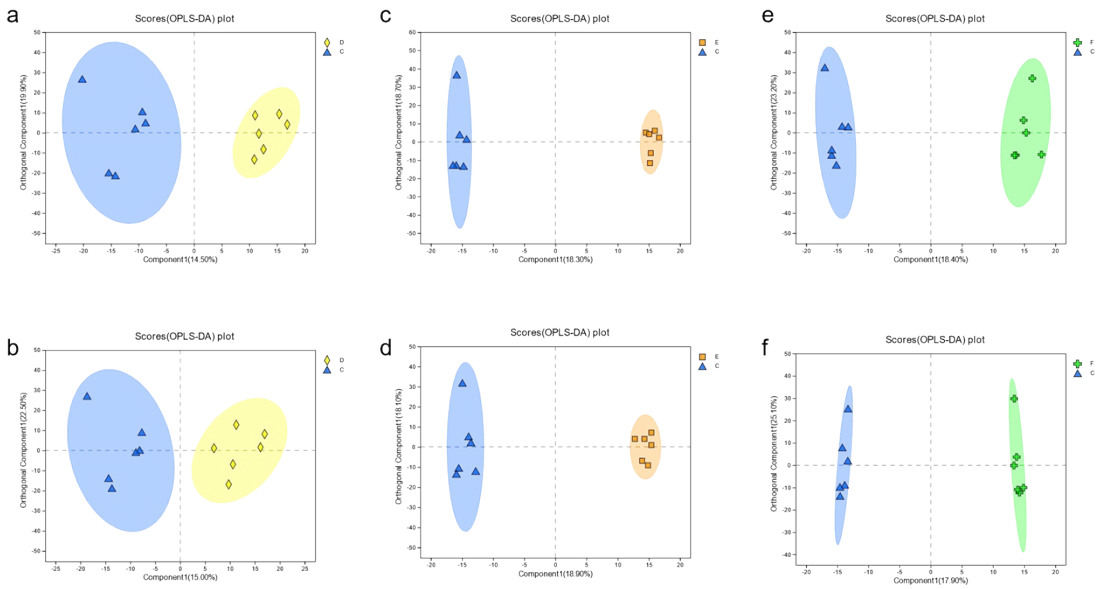

Figure 10: OPLS-DA scatter plots of 24-h urine in pos (a/c/e) and neg (b/d/f) modes comparing each ACN intervention group with the MPTP group. C is the MPTP group, D is the ACN50+MPTP group, E is the ACN100+MPTP group, and F is the ACN200+MPTP group.

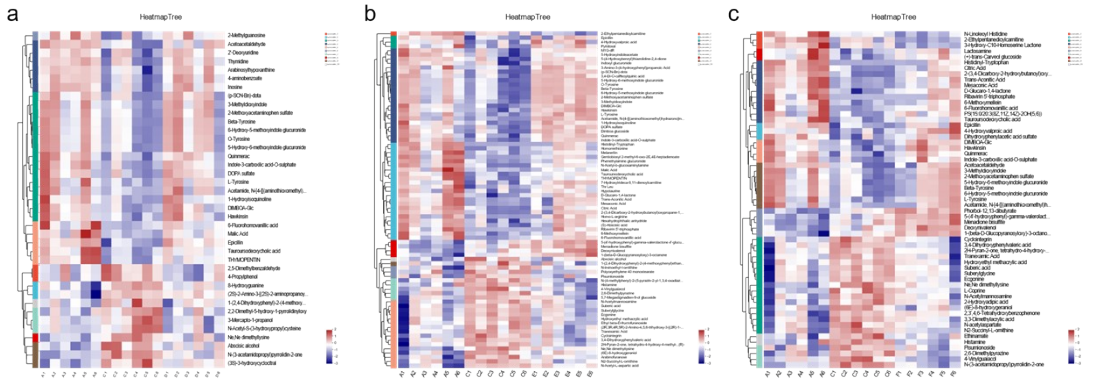

Figure 11: Cluster heat maps of PD urine metabolites in (a) ACN50 group, (b) ACN100 group and (c) ACN200 group, respectively.

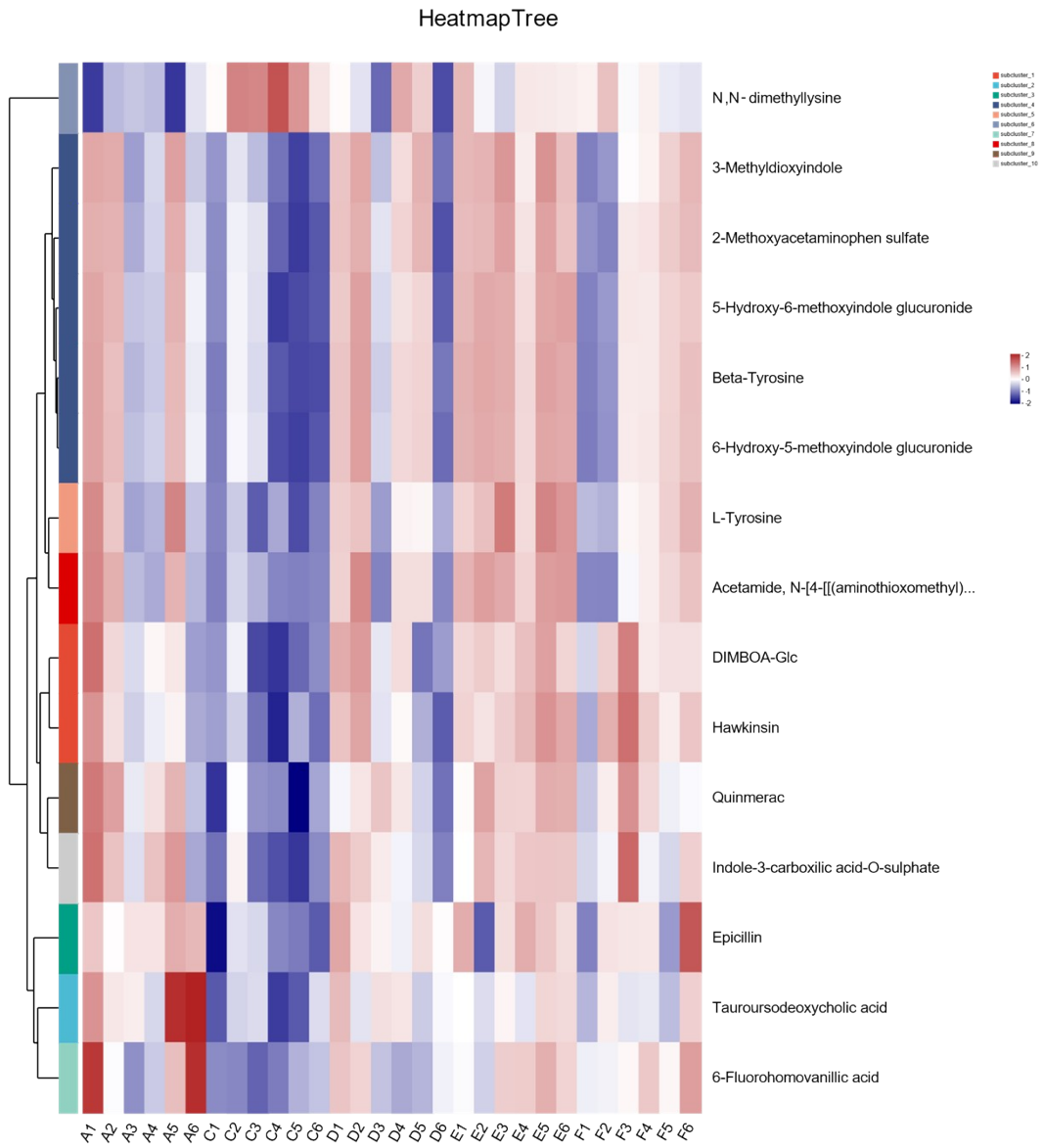

Figure 12: Clustering heatmaps of key urine differential metabolites of ACN against PD. A is the negative control group, C is the MPTP group, D is the ACN50+MPTP group, E is the ACN100+MPTP group, and F is the ACN200+MPTP group. n=6 mice per group.

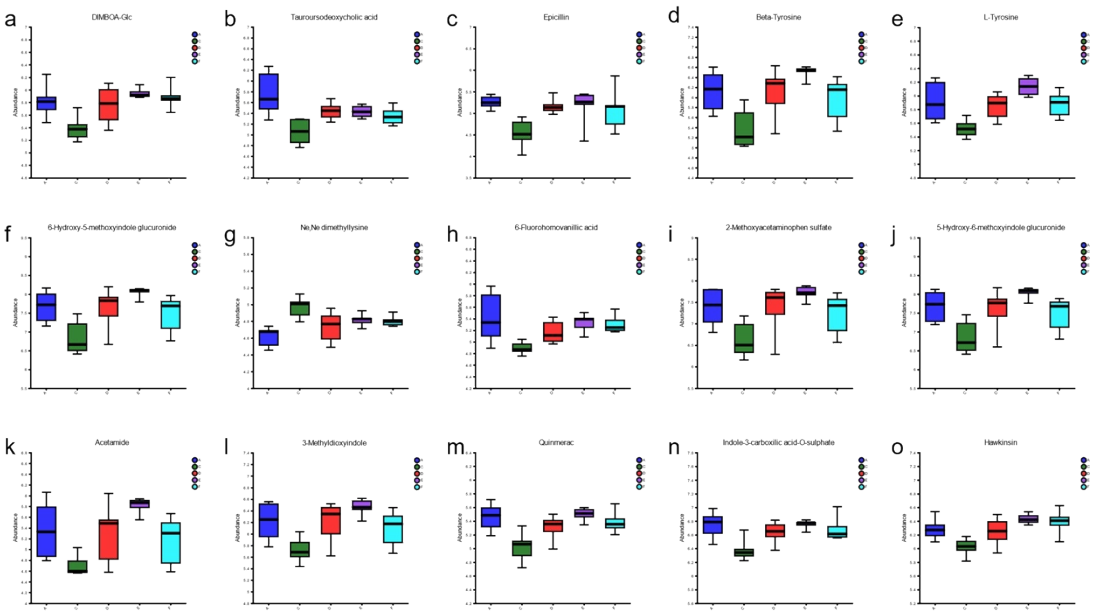

Figure 13: Box diagram of key differential metabolites in 24h urine of ACN with effect on PD-like phenotype mice. A is the negative control group, C is the MPTP group, D is the ACN50+MPTP group, E is the ACN100+MPTP group, and F is the ACN200+MPTP group.

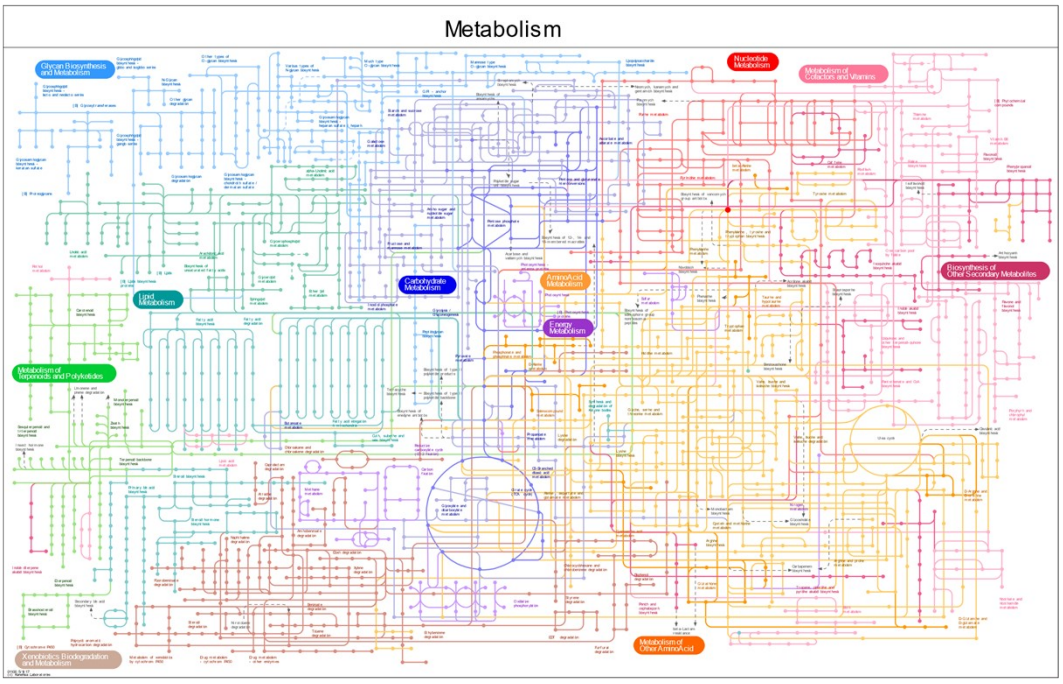

Figure 14: iPth plots of key urine differential metabolites of ACN against PD.

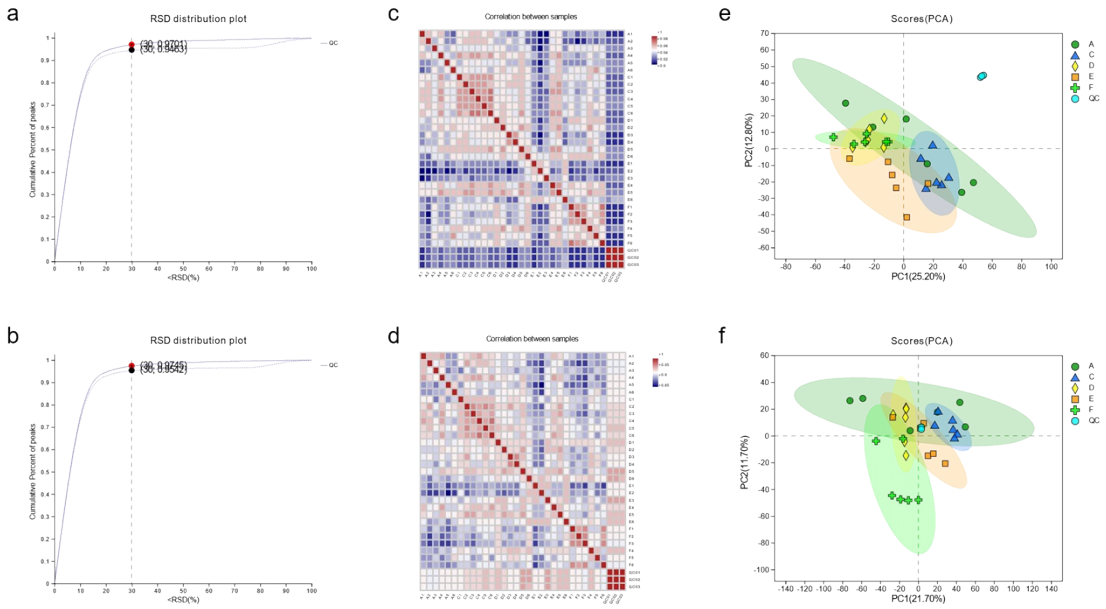

Figure 15: Analysis of serum metabolomics approach. QC sample evaluation chart under (a) pos and (b) neg mode, dashed line indicates before pretreatment and solid line indicates after pretreatment. Sample correlation heat maps of (c) pos and (d) neg mode. (e) PLS-DA score plots of urine samples in pos and (f) neg mode. A is the negative control group, C is the MPTP group, D is the ACN50+MPTP group, E is the ACN100+MPTP group, and F is the ACN200+MPTP group.

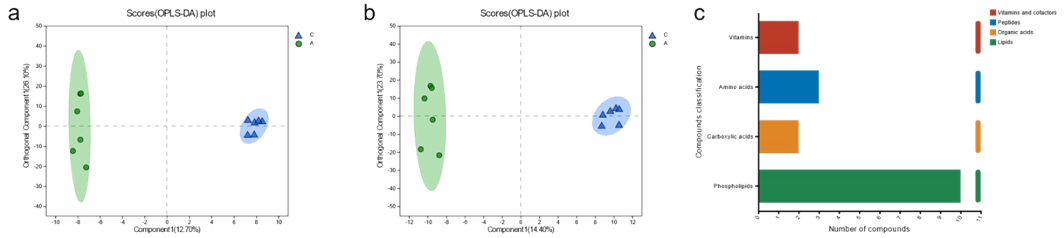

Figure 16: Serum differential metabolite screening in mice with PD-like phenotypes. (a) Plot of OPLS-DA scores in model and control groups in pos and (b) neg mode. (c) Statistical graph of KEGG compound classification. A is the negative control group, C is the MPTP group.

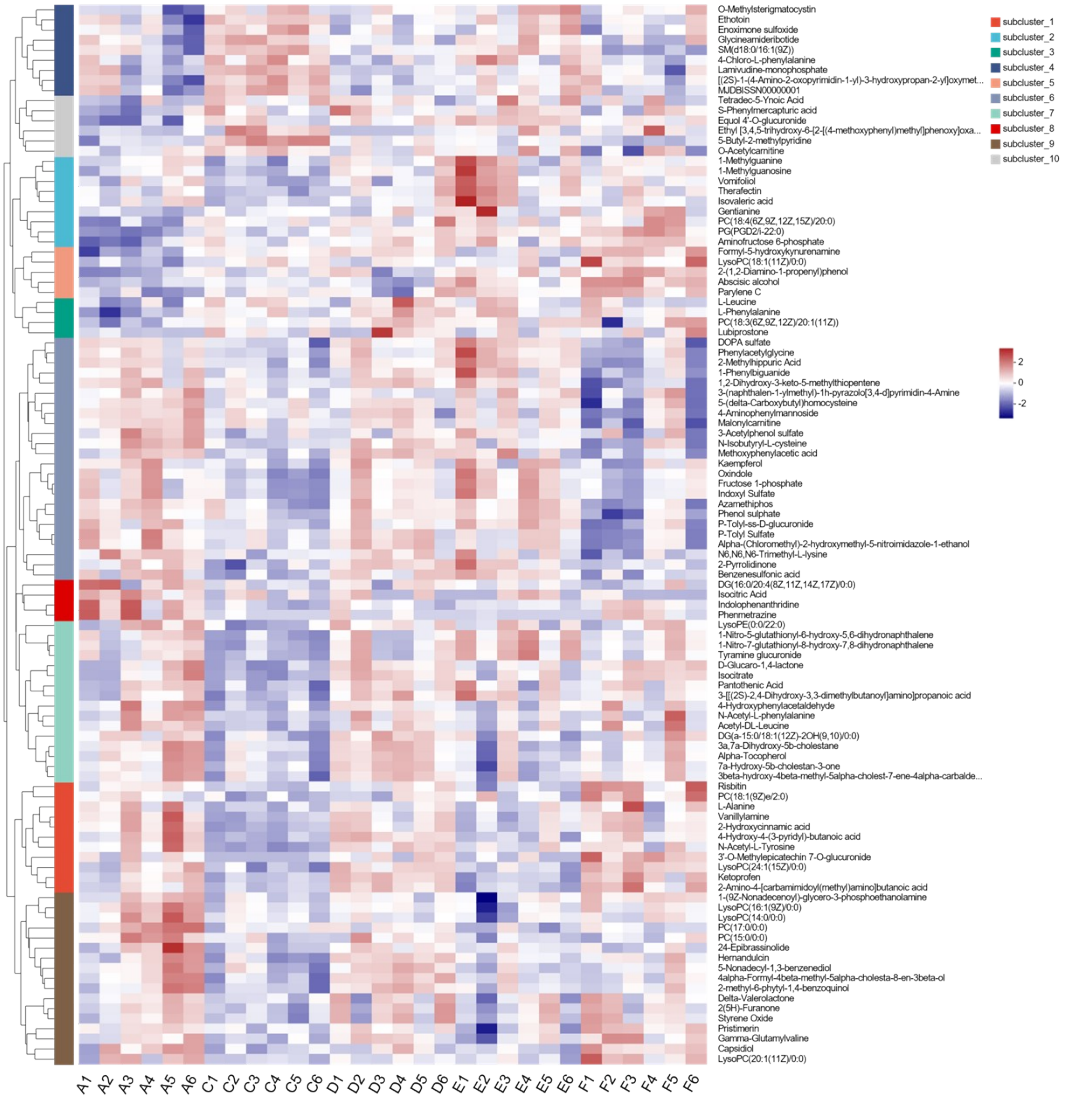

Figure 17: Clustered heatmap of PD differential serum metabolites.

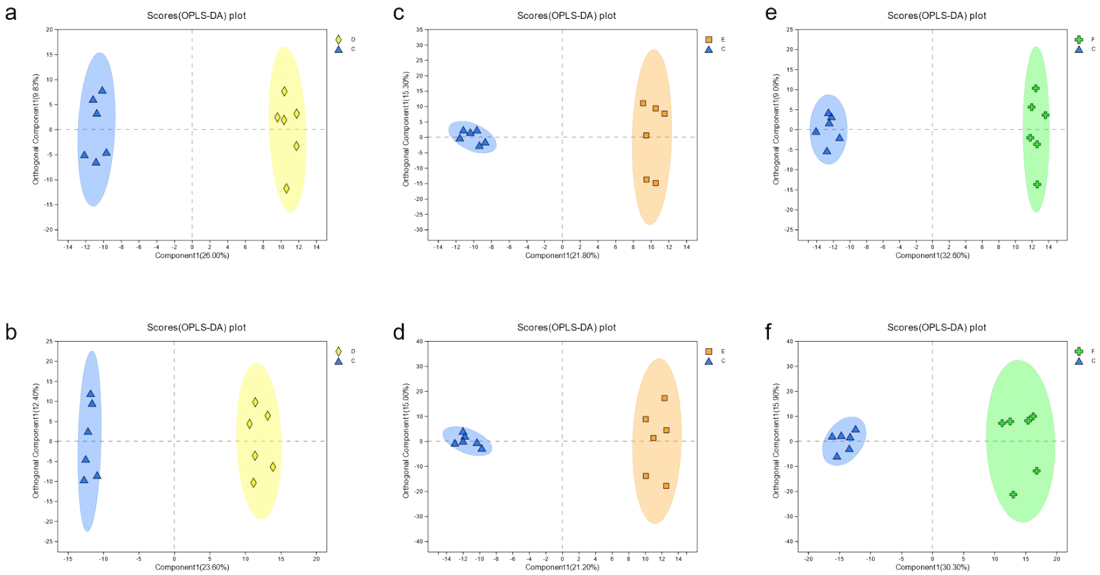

Figure 18: OPLS-DA scatter plots of serum in pos (a/c/e) and neg (b/d/f) modes comparing each ACN intervention group with the MPTP group. C is the MPTP group, D is the ACN50+MPTP group, E is the ACN100+MPTP group, and F is the ACN200+MPTP group.

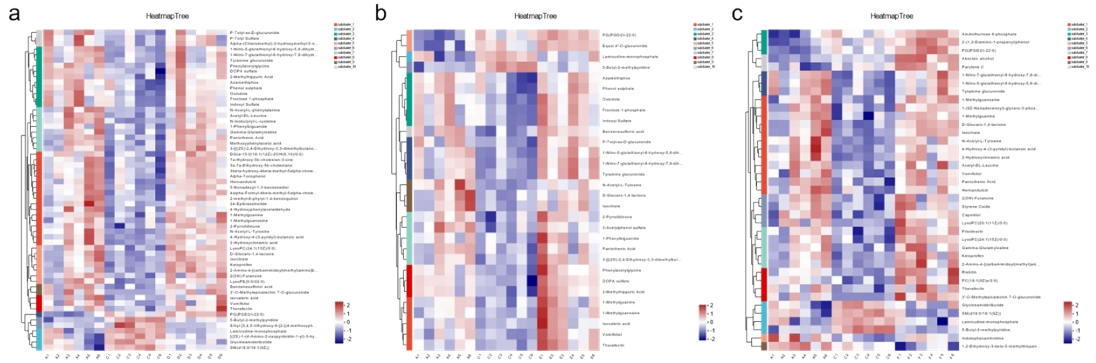

Figure 19: Cluster heat maps of PD serum metabolites in (a) ACN50 group, (b) ACN100 group and (c) ACN200 group, respectively.

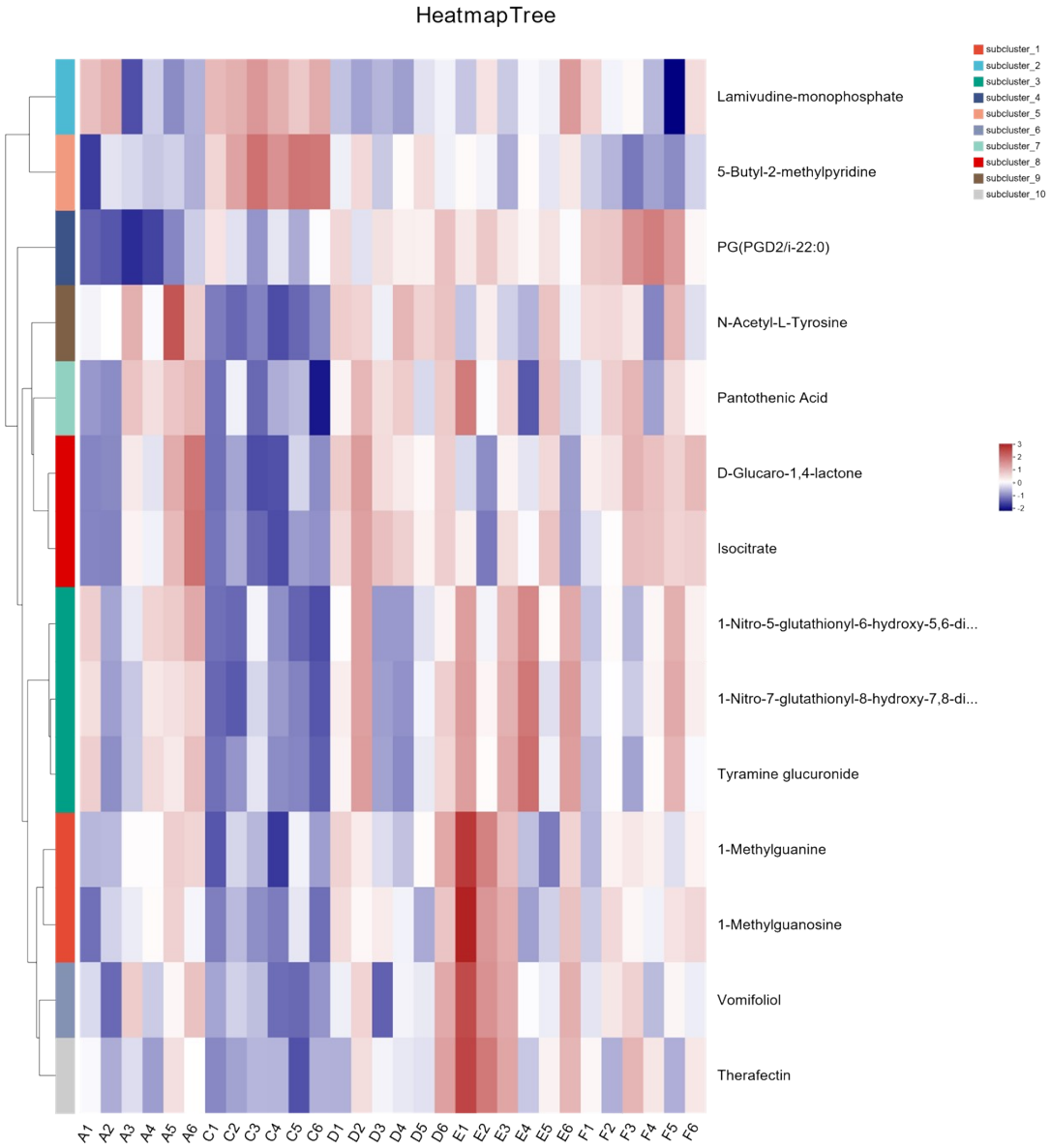

Figure 20: Clustering heatmaps of key serum differential metabolites of ACN against PD. A is the negative control group, C is the MPTP group, D is the ACN50+MPTP group, E is the ACN100+MPTP group, and F is the ACN200+MPTP group. n=6 mice per group.

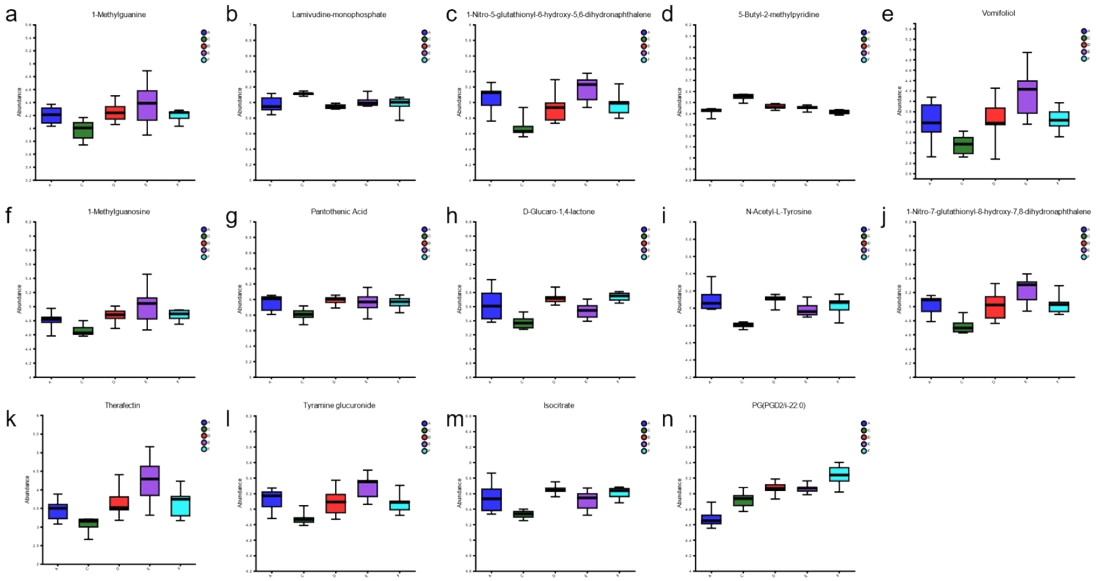

Figure 21: Box diagram of key differential metabolites in serum of ACN with effect on PD-like phenotype mice. A is the negative control group, C is the MPTP group, D is the ACN50+MPTP group, E is the ACN100+MPTP group, and F is the ACN200+MPTP group.

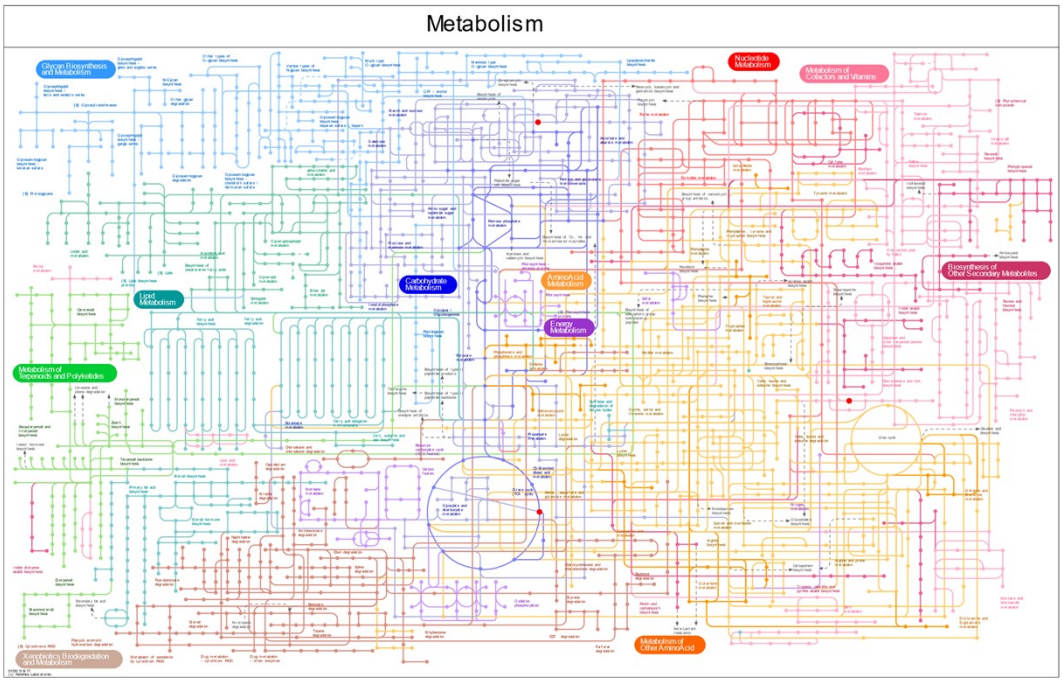

Figure 22: iPth plots of key serum differential metabolites of ACN against PD.

2. Content of ACN in crude extracts of anthocyanins of *Lycium ruthenicum* Murray

2.1 Purity of ACN

ACN was supplied by Shaanxi Qingzhi Biotechnology Company, China, with the item number 220926, and the test report form showed that the purity of the crude extract powder was 50%.

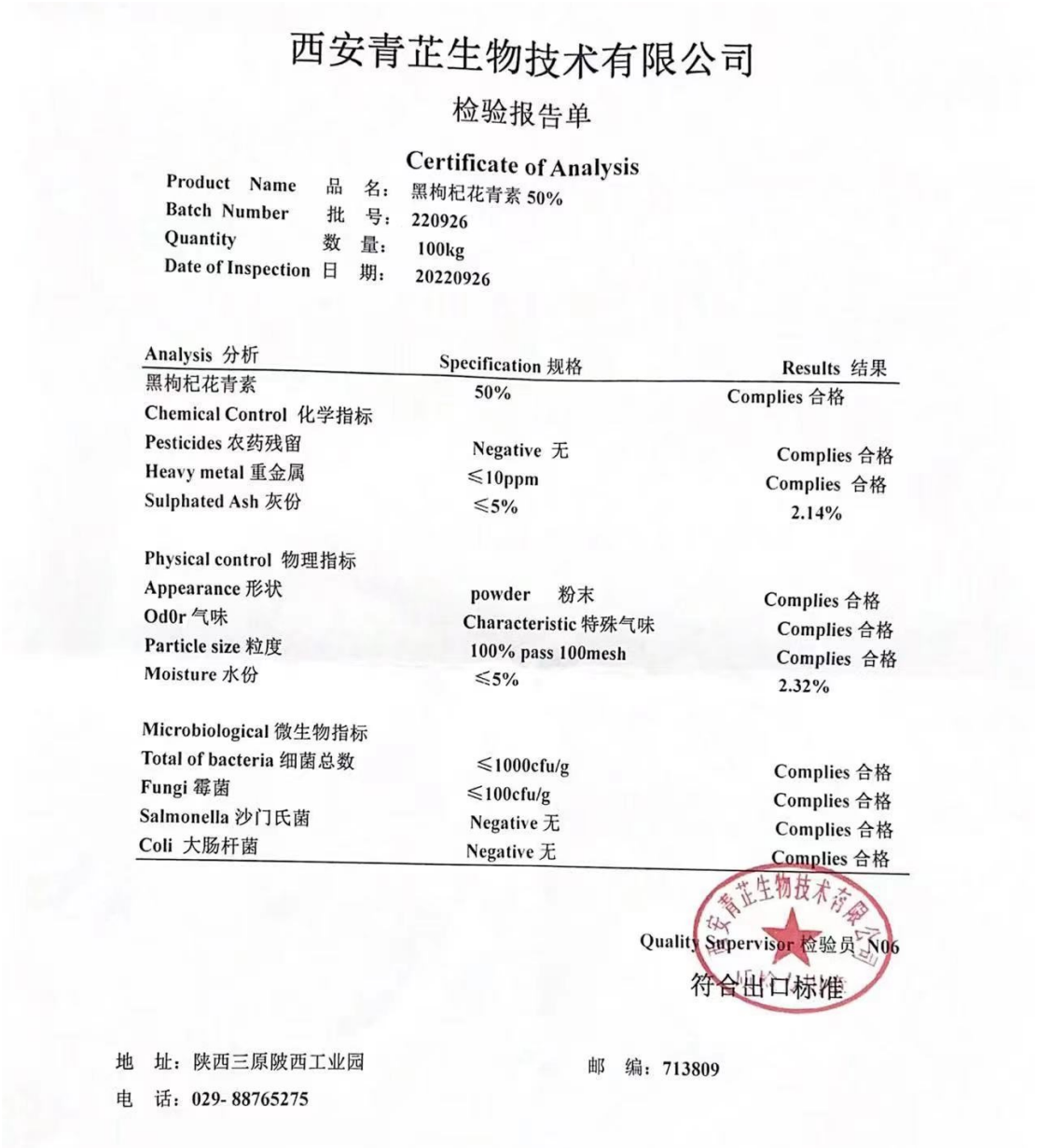

西安青芷生物技术有限公司

检验报告单

Certificate of Analysis

Product Name 品 名：黑枸杞花青素 50%
Batch Number 批 号：220926
Quantity 数 量：100kg
Date of Inspection 日 期：20220926

Analysis 分析	Specification 规格	Results 结果
黑枸杞花青素	50%	Complies 合格
Chemical Control 化学指标		
Pesticides 农药残留	Negative 无	Complies 合格
Heavy metal 重金属	≤10ppm	Complies 合格
Sulphated Ash 灰份	≤5%	2.14%
Physical control 物理指标		
Appearance 形状	powder 粉末	Complies 合格
Od0r 气味	Characteristic 特殊气味	Complies 合格
Particle size 粒度	100% pass 100mesh	Complies 合格
Moisture 水份	≤5%	2.32%
Microbiological 微生物指标		
Total of bacteria 细菌总数	≤1000cfu/g	Complies 合格
Fungi 霉菌	≤100cfu/g	Complies 合格
Salmonella 沙门氏菌	Negative 无	Complies 合格
Coli 大肠杆菌	Negative 无	Complies 合格

Quality Supervisor 检验员 N06

符合出口标准

地 址：陕西三原陂西工业园 邮 编：713809

电 话：029- 88765275

2.2 Total anthocyanin content in ACN was determined using a modified PH difference method

2.2.1 Experimental apparatus and reagents

Instruments: UV-1200 visible spectrophotometer (Shanghai Meppan Instruments Co., Ltd.), ME204E/02 electronic balance (Shanghai Mettler-Toledo Instruments Co., Ltd.)
Reagents: 0.2 mol/L KCl solution, 0.2 mol/L HCl solution, 0.2 mol/L NaAc solution, 0.1 mol/L citric acid solution, 0.1 mol/L sodium citrate solution, prepared PH1.0, PH4.5, PH3.0 buffer.

2.2.2 Experimental method

Precisely weighed 60.4 mg of the crude extract of *Lycium ruthenicum* Murray anthocyanin, added PH3.0 buffer and fixed to 50 ml, and then took 7 ml and fixed to 21 ml to get the sample solution, after standing for 10 min, the absorbance curve of ACN was obtained by scanning the partially visible wavelengths between 400-750 nm. Further, the absorbance was measured at the wavelengths of 520-530 nm to get the absorbance curve.
The sample solution was taken as 3 mL, which was fixed to 9 mL with PH1.0 and PH4.5 buffer respectively to obtain the test material. After equilibrating for a period of time, the absorbance values were measured at the maximum absorbance wavelength and 700 nm wavelength respectively, and the difference of absorbance was shown in Fig. c. It was obtained that the test material reached equilibrium after 100 min, and A=0.234.
The mass fraction of total anthocyanins was calculated according to the formula.

$$X = \frac{A * MW * DF * V}{\varepsilon * l * m * 10}$$

In the formula, X, mass fraction of total anthocyanins, g/100g; A, the difference in absorbance between the test solutions of the test samples at pH 1.0 and pH 4.5, A=(A_{maxnm}-A_{700nm})pH 1.0-($A_{max\ nm}$-A_{700nm})pH 4.5; Mw, the average molar mass of the mixed anthocyanins, g/mol; DF is the dilution factor; V, total volume of the extraction solution, V/(mL); ε, the average molar extinction coefficient of the mixed anthocyanins, L/(mol-cm); l, thickness of the cuvette, cm; m, mass of the weighed sample, g; V, total volume of the extract, V/(mol-cm); V, total volume of the extracted sample, V mL; ε, average molar extinction coefficient of mixed anthocyanins, L/(mol-cm); l, thickness of cuvette, cm; m, mass of weighed sample, g; 10, conversion factor from g/kg to g/100g.

2.2.3 Experimental results

The maximum absorption wavelength of the prepared sample was 523 nm as shown in Figures a-b. From Figure c, the sample reached stabilisation after 100 min of equilibration with A=0.234. The

total anthocyanin content was calculated to be 5.82 g/100g according to the formula.

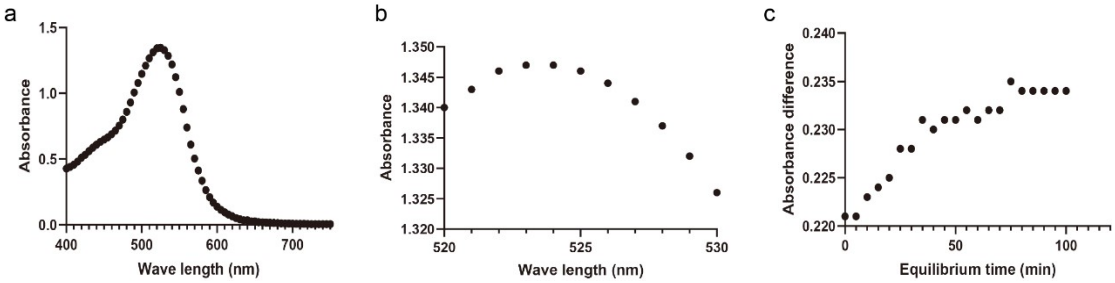

Note: (a) and (b) are the absorbance curves of the sample solution at 400-750 nm and 520-530 nm, respectively. (c) Difference in absorbance at 523 nm and 700 nm for the test material.